

1 **Title**

2 Projections of global delta land loss from sea-level rise in the 21st century

3 **Authors**

4 Jaap H. Nienhuis<sup>1,\*</sup>, Roderik S.W. van de Wal<sup>1,2</sup>

5 **Affiliations**

6 <sup>1</sup>Department of Physical Geography, Utrecht University, Utrecht, NL

7 <sup>2</sup>Institute for Marine and Atmospheric Research, Utrecht University, Utrecht, NL

8 \*corresponding author address: Princetonlaan 8a, 3584 CB, Utrecht, [j.h.nienhuis@uu.nl](mailto:j.h.nienhuis@uu.nl)

9 **Key points**

- 10 • Model of river delta response to sea level rise and river sediment applied to 6,402 deltas and  
11 tested against land area change observations
- 12 • Projections suggest net delta land loss for GMSLR > 5.5 mm/yr, and for RSLR under IPCC  
13 RCP4.5 and RCP8.5 by 2100
- 14 • Climate-change driven sea-level rise will likely exceed the effects of dams and subsidence on  
15 global delta land loss by 2100

16 **Abstract**

17 River deltas will likely experience significant land loss because of relative sea-level rise (RSLR),  
18 but predictions have not been tested against observations. Here, we use global data of RSLR and  
19 river sediment supply to build a model of delta response to RSLR for 6,402 deltas, representing  
20 86% of global delta land. We validate this model against delta land area change observations  
21 from 1985-2015, and project future land area change for IPCC RSLR scenarios. For 2100, we  
22 find widely ranging delta scenarios, from  $+94 \pm 125$  (2 s.d.)  $\text{km}^2 \text{yr}^{-1}$  for RCP2.6 to  $-1026 \pm 281$   
23  $\text{km}^2 \text{yr}^{-1}$  for RCP8.5. River dams, subsidence, and sea-level rise have had a comparable influence  
24 on reduced delta growth over the past decades, but if we follow RCP8.5 to 2100, more than 85%  
25 of delta land loss will be caused by climate-change driven sea-level rise, resulting in a loss of  
26 ~5% of global delta land.

27 **Plain language summary**

28 River deltas can erode and lose land from sea-level rise. Here we make model predictions of the  
29 effects of sea-level rise for global delta land area change up to 2100. Our model is validated  
30 against observations of delta land area change from 1985-2015. For 2100, we find that most  
31 climate change scenarios lead to net delta land loss. Worst-case scenarios for 2100 lead to a  
32 global river delta land loss of ~5% of delta land, at a rate of 1000  $\text{km}^2$  per year.

### 33 **Introduction**

34 River deltas are low-lying coastal landforms created by fluvial sediment deposition. Delta  
35 shorelines can retreat landward through relative sea-level rise (RSLR) but also advance seaward  
36 through sedimentation and delta plain aggradation. These dynamics are widely acknowledged  
37 and observed in the field (Helland-Hansen, 1996; Blum & Törnqvist, 2000), in experiments  
38 (Muto, 2001; Kim et al., 2006, 2009; Lai & Capart, 2009), and in numerical simulations  
39 (Swenson, 2005; Fagherazzi & Overeem, 2007; Hoogendoorn et al., 2008; Anderson et al.,  
40 2019).

41 Currently, however, many projections of future coastal and delta change from RSLR follow a so-  
42 called “bath-tub” or passive flood mapping approach (Hinkel et al., 2014; Kulp & Strauss, 2019;  
43 Ward et al., 2020). The bath-tub approach offers high spatial detail but ignores erosion and  
44 sedimentation (Anderson et al., 2018), which is particularly relevant for river deltas. The  
45 potential deviation between bath-tub estimates and true coastal change is evident from a global  
46 analysis that shows that deltas have gained land in recent decades despite sea-level rise (Nienhuis  
47 et al., 2020). An additional challenge is that of validation (French et al., 2016). Many projections  
48 of coastal and delta change for future RSLR have not been tested against observations based on  
49 past RSLR (Schuerch et al., 2018; Vousdoukas et al., 2020).

50 From a theoretical perspective, delta morphodynamics can be viewed as a balance between  
51 fluvial sediment supply and RSLR. Fluvial sediment delivered to a delta is partitioned between  
52 delta plain aggradation, shoreline progradation, and losses further offshore (Blum & Törnqvist,  
53 2000; Kim et al., 2006; Lorenzo-Trueba et al., 2009) (Fig. 1a, 1b). RSLR and/or delta  
54 progradation creates accommodation space on the delta plain that traps fluvial sediment. Fast  
55 RSLR can force a scenario of delta retreat if all sediment is deposited on the delta plain and no  
56 sediment is left to supply the delta shoreline. Similarly, reductions in fluvial sediment supply to  
57 river deltas, resulting from e.g. dams (Dunn et al., 2019) or sand mining (Hackney et al., 2020),  
58 can decrease natural delta land gain rates (Besset et al., 2019; Nienhuis et al., 2020).

59 The objective of this study is to apply first-order delta morphodynamic principles to make  
60 improved projections of future delta change under RSLR that are compared against historical  
61 observations. Our projections consider various IPCC representative concentration pathway  
62 (RCP) scenarios for sea level rise to 2100 and assume modern-day subsidence and fluvial

63 sediment supply rates. We use a broad definition of deltas, including coastal river deposits  
 64 sometimes referred to as estuaries or strandplains, and apply our methods on a global scale. This  
 65 allows us to compare delta dynamics under a wide range of RSLR and fluvial sediment supply  
 66 conditions and investigate drivers and trends that would be obscured in studies considering only  
 67 a single delta.

## 68 **Methods**

69 We have developed a simple morphodynamic model to project land area change of 6,402 deltas  
 70 (Fig. 1c) for various sea-level rise scenarios. Our model compares fluvial sediment supply  
 71 against local subsidence and sea-level rise, which together constitute RSLR. Based on the  
 72 present-day delta area, we follow a morpho-kinematic approach (Wolinsky, 2009) to predict  
 73 delta land loss (Fig. 1a) or gain (Fig. 1b),

$$74 \quad \frac{dA_{\text{delta}}}{dt} = \frac{f_r \cdot Q_{\text{river}} - \frac{1}{2} A_{\text{delta}} \cdot \text{RSLR}}{D_f}, \quad (1)$$

75 where  $A_{\text{delta}}$  is the river delta area ( $\text{m}^2$ ),  $dA_{\text{delta}}/dt$  is the change in river delta area ( $\text{m}^2 \text{yr}^{-1}$ ),  $Q_{\text{river}}$   
 76 is the fluvial sediment flux ( $\text{m}^3 \text{yr}^{-1}$ ),  $f_r$  is the fraction of the fluvial sediment retained in the delta  
 77 profile, RSLR is the relative sea level rise rate ( $\text{m yr}^{-1}$ ), and  $D_f$  is the delta foreset depth (m). The  
 78 fraction  $\frac{1}{2}$  arises from our triangular approximation of delta area (Fig. 1). Shoreline changes  
 79 scale with delta width at the shoreline, whereas the average delta width between the apex and the  
 80 shoreline is half that amount.

81 Our model is one of the simplest possible models for delta change that includes its two main  
 82 drivers, base level change (RSLR) and fluvial sediment supply. We apply it as a time-  
 83 independent model, where changes are instantaneous and do not compound (i.e., delta area is not  
 84 updated at a next timestep). We ignore delta land gain along the upstream boundary in our  
 85 assessment of delta land area change because it constitutes land conversion from existing (albeit  
 86 non-deltaic) land. We apply this model to 6,402 deltas, a subset from Nienhuis et al. (2020),  
 87 because of additional requirements to delta morphology further specified in the supplemental  
 88 materials.

89 We retrieve global suspended load fluvial sediment supply for 6,402 deltas from WBMSed  
 90 (Cohen et al., 2014; Nienhuis et al., 2020) and convert it to a depositional sediment flux using a

91 bulk density ( $1600 \text{ kg m}^{-3}$ ). WBMSed considers two fluvial sediment scenarios, pristine ( $Q_{river}^p$ )  
92 and disturbed ( $Q_{river}^d$ ), that represent historic (before human impact) and modern conditions,  
93 respectively. For our future projections of delta change we assume modern, disturbed fluvial  
94 sediment supply conditions.

95 We estimate delta area as a triangle defined by the delta apex and its lateral shoreline extent. For  
96 1081 large deltas that represent 81% of global delta area, we use the manually collected delta  
97 apex and shoreline extent from Edmonds et al (2020). We extend our dataset beyond these to  
98 include a wide range of morphologies, RSLR rates, and local environments. For 5321 other,  
99 mostly smaller deltas, we estimate the lateral shoreline extent using the delta area proxy from  
100 Syvitski and Saito (2007), and we estimate the delta length (shoreline to delta – basement  
101 transition) from its sedimentary wedge by fitting a basement cross-sectional profile under  
102 SRTM15+ elevation data (Fig. 1d). We use the depth of the basement profile under the modern  
103 river mouth as a measure of the delta foreset depth ( $D_f$ ).

104 We obtain measures of RSLR from various sources. For historic conditions, we use regional (1  
105 degree) sea-level reconstructions from 1985-2015 (Dangendorf et al., 2019) combined with local  
106 vertical land movement (uplift, subsidence) observations based on GPS stations nearest to each  
107 delta (Blewitt et al., 2018; Shirzaei et al., 2021). For future projections (2007-2100), we use  
108 IPCC SROCC scenarios for RCP2.6, 4.5, and 8.5 (Oppenheimer et al., 2019) and assume land  
109 subsidence remains unchanged from their modern rates (2000-2014).

110 We assess model and data uncertainty by means of a Monte Carlo method and a sensitivity  
111 analysis, further details can be found in the supplementary materials. Model data and code  
112 necessary to reproduce the results are freely available online.

### 113 **Test against observations**

114 We test our morphodynamic model against observed delta area change from 1985-2015, using  
115 the average of two global land-water change models (Donchyts et al., 2016; Pekel et al., 2016).  
116 Both models are based on Landsat 30 m imagery (NASA, 2020) and are processed in the Google  
117 Earth Engine environment (Gorelick et al., 2017); we sum the outcomes within individual delta  
118 area extents for 6,402 deltas as defined by Nienhuis et al (2020). We find that our delta area  
119 change predictions are generally in the correct order of magnitude (Fig. 2), and that it explains a

120 substantial fraction ( $R^2 = 0.39$ ,  $MSRD = 0.6 \text{ km}^2 \text{ yr}^{-1}$ ) of observed delta land loss and land gain.  
121 Part of the past trend might still be too small to be explained by the two processes captured in  
122 our model. Land area change observations are also uncertain. Overall, there is positive bias in  
123 our global land change predictions when we use a sediment fraction retained ( $f_r$ ) of 1, predicting  
124 a net gain of  $330 \text{ km}^2 \text{ yr}^{-1}$  vs. observations of  $196 \text{ km}^2 \text{ yr}^{-1}$ . For our future projections we use  $f_r =$   
125 0.9 to more closely match observed and predicted global net land gain for the period 1985-2015.

### 126 **Predictions of future delta change**

127 Future deltas will generally experience increased RSLR rates (Fig. 3a), with implications for  
128 delta area change. Assuming a globally constant RSLR and modern fluvial sediment supply, we  
129 find that global deltas gain land for a RSLR rate below  $\sim 5.5 \text{ mm yr}^{-1}$  (Fig. 3b). Global delta land  
130 area will decrease if that rate is exceeded.

131 Delta area change is also affected by modifications to the fluvial sediment supply. Comparing  
132 modern supply against pristine (before river dams or deforestation (Cohen et al., 2014) fluvial  
133 sediment supply to deltas, we find that the global change in sediment fluxes have had a small but  
134 noticeable effect (Fig. 3b). Without anthropogenic modifications to the sediment supply feeding  
135 deltas, the threshold for net global delta land loss would have been  $6.5 \text{ mm yr}^{-1}$ . The comparative  
136 effect of fluvial sediment supply changes to global deltas can be further appreciated by a back-  
137 of-the envelope calculation: the global human-induced fluvial sediment flux reduction ( $1.4$   
138  $\text{BT/yr}$ , Syvitski et al., 2005) distributed across all global deltas ( $850,000 \text{ sq. km}$ , Edmonds et al.,  
139 2020) is equivalent to  $\sim 1 \text{ mm yr}^{-1}$  of RSLR ( $1.4 \cdot 10^{12} / 1600 / 850 \cdot 10^9$ ). This modest effect is  
140 partially because deforestation cancels out river dams on this global scale – resulting trends for  
141 individual deltas vary considerably.

142 In the limit of no fluvial sediment supply, our model predictions simplify to gradual upslope  
143 delta migration, with the slope given by the delta foreset depth over delta length (Fig. 3b). Such  
144 projections would estimate delta land loss of  $-440 \text{ km}^2 \text{ yr}^{-1}$  for 1985-2015, contrasting observed  
145 delta land gain of  $+196 \text{ km}^2 \text{ yr}^{-1}$ .

146 Future RSLR will vary regionally and depends on the RCP scenario. Following the recent  
147 SROCC projections for sea-level rise under RCP8.5 (Oppenheimer et al., 2019) and assuming  
148 fluvial sediment supply and subsidence rates remain unchanged, we find global delta land loss

149 rates of  $1026 \pm 281 \text{ km}^2 \text{ yr}^{-1}$  (2 s.d.) by the end of the century (2081-2100). Cumulative since  
150 2007 to 2100, sea level rise under RCP8.5 will lead to the disappearance of about  $37,178 \pm$   
151  $17,919 \text{ km}^2$  (2 s.d.) of deltaic land – equal to about 5% of total delta area.

152 Projected land area change will vary between deltas (Fig. 4). Despite the general trend of  
153 increasing land loss for higher RSLR, the specific RSLR threshold that triggers a delta into land  
154 loss is highly variable. Some deltas are projected to sustain growth under all RCP scenarios.  
155 Low-gradient mega-deltas are more sensitive to RSLR, the rapid land gain observed in Southeast  
156 Asia and South America (Nienhuis et al., 2020) will diminish under all RCP scenarios (Fig. 4b-  
157 d).

158 Arctic deltas experience, on average, less RSLR because of ongoing glacial isostatic adjustment  
159 and gravitational effects. Land losses are projected to be larger, under all RCP scenarios, because  
160 they receive less sediment relative to their surface area. However, Arctic deltas will also  
161 experience many other effects of climate change that are not captured in our morphodynamic  
162 model (Barnhart et al., 2016; Lauzon et al., 2019). In general, our projections for individual  
163 deltas are highly uncertain and should be interpreted with caution (Thieler et al., 2000).

#### 164 **Drivers of future delta land area change**

165 We also assess the relative importance of various drivers of delta change. First, model results of  
166 an uninhibited growth scenario, without sea-level rise, river damming, deforestation, or  
167 subsidence, suggests a global gain about  $758 \text{ km}^2 \text{ yr}^{-1}$  (Fig. 5a). This rate is higher than what  
168 would be expected for long-term delta growth: modern total delta area ( $\sim 900,000 \text{ km}^2$ ) divided  
169 by the age of modern delta initiation ( $\sim 7000 \text{ yr}$ ) (Stanley & Warne, 1994) suggests a long-term  
170 average delta land area gain of about  $130 \text{ km}^2 \text{ yr}^{-1}$ .

171 Modern observed delta land gain of  $196 \text{ km}^2 \text{ yr}^{-1}$  is substantially lower than the uninhibited delta  
172 growth case (Fig. 5a). We distinguish four drivers affecting delta growth: dams, deforestation,  
173 subsidence, and SLR, and compute expected delta area change if only one of these drivers were  
174 present. Model results suggests that, of those four drivers, sea-level rise has dominated the  
175 observed reduction in delta land gain from 1985-2015 compared to uninhibited conditions (Fig.  
176 5a). Note however that our assessment only includes fluvial suspended sediment load and not

177 bedload, which adds to the total fluvial sediment load and responds differently to river dams  
178 (Kondolf, 1997; Nittrouer & Viparelli, 2014).

179 Climate-change driven sea-level rise is expected to continue to dominate river delta land loss. By  
180 the end of the century, sea-level rise under all RCP scenarios will greatly exceed other global  
181 drivers of delta land loss (Fig. 5b).

## 182 **RSLR control on delta morphology**

183 Besides a reduction of delta area, RSLR also affects delta plan-view morphology through its  
184 influence on the partitioning of fluvial sediment between delta topset, foreset, and bottomset  
185 (Blum & Törnqvist, 2000; Jerolmack, 2009; Kim et al., 2009). RSLR increases accommodation  
186 space and sediment deposition on the delta plain and lowers sediment delivery to the river mouth  
187 (Kim et al., 2009), which can make a delta more wave- or tide-dominated (Nienhuis et al., 2020).

188 Our model suggests that for a global mean RSLR of  $10 \text{ mm yr}^{-1}$ , the rate of delta plain  
189 accommodation space creation is equivalent to about 80% of the global fluvial sediment flux  
190 (Fig. 6a). Such a RSLR rate would leave 20% of the fluvial sediment supply available at the river  
191 mouth for redistribution along present-day coasts. RSLR and delta response to RSLR varies  
192 between deltas: following our model predictions for RCP8.5 by 2100, we predict that 20% of all  
193 coastal deltas will be in forced retreat (abandoned of all fluvial sediment supply at the river  
194 mouth). RSLR rates from 1985-2015 have trapped 20% of the global fluvial sediment supply  
195 onto the delta plain, in addition to delta sediment trapping that results from delta progradation.  
196 This will increase to 60% by 2100 if emissions follow RCP8.5, a high-end scenario. The slope of  
197 the sediment flux curve (in blue) exceeds the slope of the fraction of deltas curve (in red),  
198 indicating that large deltas are more strongly affected by RSLR (Fig. 6a).

199 Using a new model for river delta morphology (Nienhuis et al., 2020), we can investigate  
200 potential plan-view effects of RSLR-induced sediment trapping on the delta plain (Fig. 6b). A  
201 decrease in fluvial sediment supply that arrives at the river mouth results in a shift in the river  
202 mouth sediment balance towards tidal and wave-driven sediment flows. Following our model  
203 simulations for RCP8.5 by 2100, we predict that 10% of all river-dominated deltas will transform  
204 to wave- or tide-dominated deltas, although it does not specify a rate of change for delta  
205 morphology.

## 206 **Discussion and Conclusions**

207 Our simplified delta area change model captures broad global patterns and can be tested against  
208 global observations. Accurate predictions for individual deltas remain challenging. Human-  
209 landscape interactions, most notably the construction of flood protection defenses, have had, and  
210 will have, a significant effect on delta sedimentation and their (short-term) response to RSLR.  
211 Human-landscape interactions also challenge the accurate observations of delta morphodynamics  
212 (Besset et al., 2019). Prediction accuracy is limited because of uncertainties in estimates of  
213 subsidence rates over time, sea-level change, fluvial sediment flux, and present-day morphology.  
214 Fluvial sediment supply and subsidence rates are unlikely to remain the same into the future.  
215 River damming is projected to overtake deforestation to further reduce fluvial sediment supply to  
216 deltas (Dunn et al., 2019). Population pressure and associated groundwater withdrawal will  
217 likely increase subsidence rates in many densely populated deltas (Keogh & Törnqvist, 2019;  
218 Herrera-García et al., 2021). At the same time adaptation measures may reduce subsidence rates  
219 in areas which are already under pressure.

220 Other uncertainties stem from model assumptions. We assume a linear delta response to RSLR  
221 and sediment supply. Such a response may be justified for predictions on short timescales (~100  
222 yrs) relative to the age of river deltas (~7500 yrs) (Lorenzo-Trueba et al., 2009). On the other  
223 hand, we also assume that delta morphodynamics can be expressed by a morpho-kinematic mass  
224 balance approach –an assumption that typically only holds for long timescales or for small  
225 deltas. On short timescales, land area change from individual coastal and river floods (Ward et  
226 al., 2020) or autogenic (free) delta morphodynamics such as avulsions or channel migration  
227 would likely obscure allogenic (forced) change (Li et al., 2016) of an individual delta. Future  
228 model projections should aim to be more spatially explicit, such as those by Vousdoukas et al  
229 (2020), and indicate where within deltas land area change is likely to occur.

230 Our uncertainty assessment combines data and model errors and shows that our predictions are  
231 relatively robust when applied on a global scale. Additionally, our methods and data presented  
232 here provide quantitative and morphodynamic projections that offer an improvement over  
233 frequently used bath-tub models and agree with historic data on delta land area change. Together  
234 with studies such as those by Bamunawala et al (2020), who apply similar methods to tidal inlets,

235 it shows the potential use of simplified, morphodynamic models for the characterization of future  
236 coastal change.

237 Our predictions show substantial risk of land loss from climate-change driven RSLR. We  
238 estimate that RSLR under RCP8.5 (a high-end scenario, Hausfather & Peters, 2020), will lead to  
239 the disappearance of about  $37,178 \pm 17,919$  km<sup>2</sup> of deltaic land – equal to about 5% of total delta  
240 area. Delta top sedimentation can also lead to widespread wave and tidal reworking of deltas.  
241 There are also other risks to deltas driven by RSLR that are not included in this study, such as  
242 increased coastal flooding, salinity intrusion, and river flooding.

243 Many RSLR-driven risks to river deltas, including the land loss discussed in this study, can be  
244 reduced with appropriate management strategies that support efficient use of the available  
245 sediment. Delta plain sedimentation strategies such as river diversions are a good example (Paola  
246 et al., 2011). Our results highlight that these approaches can protect deltas against some of the  
247 consequences of climate-change driven RSLR and should be encouraged.

## 248 **Acknowledgments**

249 We thank Sönke Dangendorf for sharing the RSLR reconstructions and Jorge Lorenzo-Trueba  
250 for helpful conversations about sea-level rise and deltas. We appreciate the constructive  
251 reviewing by Brad Murray and an anonymous reviewer, and editorial work from Kathleen  
252 Donohue. This research was supported by NSF award EAR-1810855 and NWO award  
253 VI.Veni.192.123 to JHN and benefitted from the Water, Climate, Future Deltas program of  
254 Utrecht University. Model code and data to reproduce the findings and figures are available via  
255 OSF (doi:10.17605/OSF.IO/R4U8K).

## 256 **References**

- 257 Anderson, T. R., Fletcher, C. H., Barbee, M. M., Romine, B. M., Lemmo, S., & Delevaux, J. M.  
258 S. M. S. (2018). Modeling multiple sea level rise stresses reveals up to twice the land at risk  
259 compared to strictly passive flooding methods. *Scientific Reports*, 8(1), 14484.  
260 <https://doi.org/10.1038/s41598-018-32658-x>
- 261 Anderson, W., Lorenzo-Trueba, J., & Voller, V. (2019). A geomorphic enthalpy method:  
262 Description and application to the evolution of fluvial-deltas under sea-level cycles.  
263 *Computers & Geosciences*, 130(May), 1–10. <https://doi.org/10.1016/j.cageo.2019.05.006>

- 264 Bamunawala, J., Dastgheib, A., Ranasinghe, R., van der Spek, A., Maskey, S., Murray, A. B., ...  
265 Sirisena, T. A. J. G. (2020). A Holistic Modeling Approach to Project the Evolution of  
266 Inlet-Interrupted Coastlines Over the 21st Century. *Frontiers in Marine Science*, 7.  
267 <https://doi.org/10.3389/fmars.2020.00542>
- 268 Barnhart, K. R., Miller, C. R., Overeem, I., & Kay, J. E. (2016). Mapping the future expansion of  
269 Arctic open water. *Nature Climate Change*, 6(3), 280–285.  
270 <https://doi.org/10.1038/nclimate2848>
- 271 Besset, M., Anthony, E. J., & Bouchette, F. (2019). Multi-decadal variations in delta shorelines  
272 and their relationship to river sediment supply: An assessment and review. *Earth-Science*  
273 *Reviews*, 193(November 2018), 199–219. <https://doi.org/10.1016/j.earscirev.2019.04.018>
- 274 Blewitt, G., Hammond, W., & Kreemer, C. (2018). Harnessing the GPS Data Explosion for  
275 Interdisciplinary Science. *Eos*, 99. <https://doi.org/10.1029/2018EO104623>
- 276 Blum, M. D., & Törnqvist, T. E. (2000). Fluvial responses to climate and sea-level change: a  
277 review and look forward. *Sedimentology*, 47(s1), 2–48. [https://doi.org/10.1046/j.1365-](https://doi.org/10.1046/j.1365-3091.2000.00008.x)  
278 [3091.2000.00008.x](https://doi.org/10.1046/j.1365-3091.2000.00008.x)
- 279 Cohen, S., Kettner, A. J., & Syvitski, J. P. M. (2014). Global suspended sediment and water  
280 discharge dynamics between 1960 and 2010: Continental trends and intra-basin sensitivity.  
281 *Global and Planetary Change*, 115, 44–58. <https://doi.org/10.1016/j.gloplacha.2014.01.011>
- 282 Dangendorf, S., Hay, C., Calafat, F. M., Marcos, M., Piecuch, C. G., Berk, K., & Jensen, J.  
283 (2019). Persistent acceleration in global sea-level rise since the 1960s. *Nature Climate*  
284 *Change*, 9(9), 705–710. <https://doi.org/10.1038/s41558-019-0531-8>
- 285 Donchyts, G., Baart, F., Winsemius, H., Gorelick, N., Kwadijk, J., & van de Giesen, N. (2016).  
286 Earth's surface water change over the past 30 years. *Nature Climate Change*, 6(9), 810–  
287 813. <https://doi.org/10.1038/nclimate3111>
- 288 Dunn, F. E., Darby, S. E., Nicholls, R. J., Cohen, S., Zarfl, C., & Fekete, B. M. (2019).  
289 Projections of declining fluvial sediment delivery to major deltas worldwide in response to  
290 climate change and anthropogenic stress. *Environmental Research Letters*, 14(8), 084034.

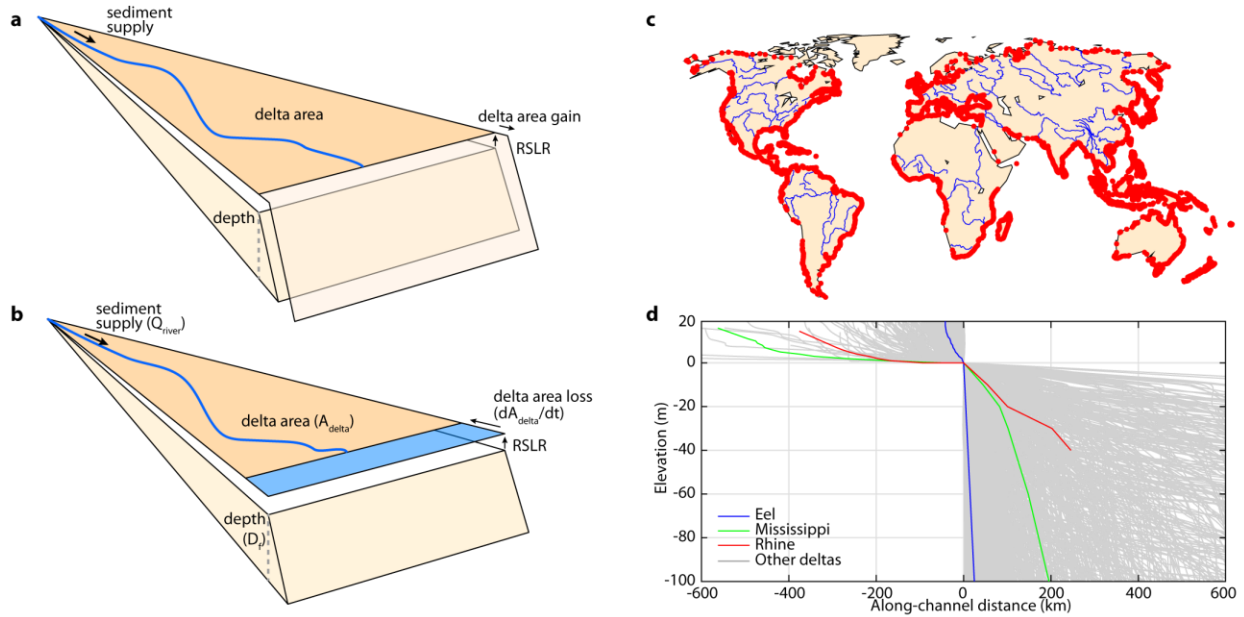
- 291 <https://doi.org/10.1088/1748-9326/ab304e>
- 292 Edmonds, D. A., Caldwell, R. L., Brondizio, E. S., & Siani, S. M. O. (2020). Coastal flooding  
293 will disproportionately impact people on river deltas. *Nature Communications*, *11*(1), 4741.  
294 <https://doi.org/10.1038/s41467-020-18531-4>
- 295 Fagherazzi, S., & Overeem, I. (2007). Models of deltaic and inner continental shelf landform  
296 evolution. *Annu. Rev. Earth Planet. Sci.*, *35*, 685–715.
- 297 French, J., Payo, A., Murray, B., Orford, J., Eliot, M., & Cowell, P. (2016). Appropriate  
298 complexity for the prediction of coastal and estuarine geomorphic behaviour at decadal to  
299 centennial scales. *Geomorphology*, *256*, 3–16.  
300 <https://doi.org/10.1016/j.geomorph.2015.10.005>
- 301 Gorelick, N., Hancher, M., Dixon, M., Ilyushchenko, S., Thau, D., & Moore, R. (2017). Google  
302 Earth Engine: Planetary-scale geospatial analysis for everyone. *Remote Sensing of*  
303 *Environment*, *202*, 18–27. <https://doi.org/10.1016/j.rse.2017.06.031>
- 304 Hackney, C. R., Darby, S. E., Parsons, D. R., Leyland, J., Best, J. L., Aalto, R., ... Houseago, R.  
305 C. (2020). River bank instability from unsustainable sand mining in the lower Mekong  
306 River. *Nature Sustainability*, *3*(3), 217–225. <https://doi.org/10.1038/s41893-019-0455-3>
- 307 Hausfather, Z., & Peters, G. P. (2020). Emissions – the ‘business as usual’ story is misleading.  
308 *Nature*, *577*(7792), 618–620. <https://doi.org/10.1038/d41586-020-00177-3>
- 309 Helland-Hansen, O. J. M. W. (1996). Shoreline Trajectories and Sequences: Description of  
310 Variable Depositional-Dip Scenarios. *SEPM Journal of Sedimentary Research*, *Vol. 66*(4),  
311 670–688. <https://doi.org/10.1306/D42683DD-2B26-11D7-8648000102C1865D>
- 312 Herrera-García, G., Ezquerro, P., Tomás, R., Béjar-Pizarro, M., López-Vinielles, J., Rossi, M.,  
313 ... Ye, S. (2021). Mapping the global threat of land subsidence. *Science*, *371*(6524), 34–36.  
314 <https://doi.org/10.1126/science.abb8549>
- 315 Hinkel, J., Lincke, D., Vafeidis, A. T., Perrette, M., Nicholls, R. J., Tol, R. S. J., ... Levermann,  
316 A. (2014). Coastal flood damage and adaptation costs under 21st century sea-level rise.  
317 *Proceedings of the National Academy of Sciences*, *111*(9), 3292–3297.

- 318 <https://doi.org/10.1073/pnas.1222469111>
- 319 Hoogendoorn, R. M., Overeem, I., & Storms, J. E. A. (2008). Process-response modelling of  
320 fluvio-deltaic stratigraphy. *Computers & Geosciences*, 34(10), 1394–1416.  
321 <https://doi.org/10.1016/j.cageo.2008.02.006>
- 322 Jerolmack, D. J. (2009). Conceptual framework for assessing the response of delta channel  
323 networks to Holocene sea level rise. *Quaternary Science Reviews*, 28(17–18), 1786–1800.  
324 <https://doi.org/10.1016/j.quascirev.2009.02.015>
- 325 Keogh, M. E., & Törnqvist, T. E. (2019). Measuring rates of present-day relative sea-level rise in  
326 low-elevation coastal zones: a critical evaluation. *Ocean Science*, 15(1), 61–73.  
327 <https://doi.org/10.5194/os-15-61-2019>
- 328 Kim, W., Dai, A., Muto, T., & Parker, G. (2009). Delta progradation driven by an advancing  
329 sediment source: Coupled theory and experiment describing the evolution of elongated  
330 deltas. *Water Resources Research*, 45(6), W06428. <https://doi.org/10.1029/2008WR007382>
- 331 Kim, W., Paola, C., Voller, V. R., & Swenson, J. B. (2006). Experimental Measurement of the  
332 Relative Importance of Controls on Shoreline Migration. *Journal of Sedimentary Research*,  
333 76(2), 270–283. <https://doi.org/10.2110/jsr.2006.019>
- 334 Kondolf, G. M. (1997). PROFILE: Hungry Water: Effects of Dams and Gravel Mining on River  
335 Channels. *Environmental Management*, 21(4), 533–551.  
336 <https://doi.org/10.1007/s002679900048>
- 337 Kulp, S. A., & Strauss, B. H. (2019). New elevation data triple estimates of global vulnerability  
338 to sea-level rise and coastal flooding. *Nature Communications*, 10(1), 4844.  
339 <https://doi.org/10.1038/s41467-019-12808-z>
- 340 Lai, S. Y. J., & Capart, H. (2009). Reservoir infill by hyperpycnal deltas over bedrock.  
341 *Geophysical Research Letters*, 36(8), L08402. <https://doi.org/10.1029/2008GL037139>
- 342 Lauzon, R., Piliouras, A., & Rowland, J. C. (2019). Ice and Permafrost Effects on Delta  
343 Morphology and Channel Dynamics. *Geophysical Research Letters*, 46(12), 6574–6582.  
344 <https://doi.org/10.1029/2019GL082792>

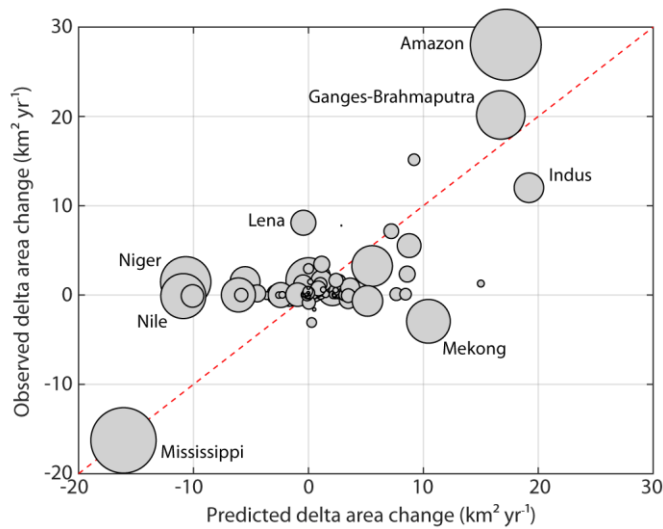
- 345 Li, Q., Yu, L., & Straub, K. M. (2016). Storage thresholds for relative sea-level signals in the  
346 stratigraphic record. *Geology*, 44(3), 179–182. <https://doi.org/10.1130/G37484.1>
- 347 Lorenzo-Trueba, J., Voller, V. R., Muto, T., Kim, W., Paola, C., & Swenson, J. B. (2009). A  
348 similarity solution for a dual moving boundary problem associated with a coastal-plain  
349 depositional system. *Journal of Fluid Mechanics*, 628, 427–443.  
350 <https://doi.org/10.1017/S0022112009006715>
- 351 Muto, T. (2001). Shoreline Autorettreat Substantiated in Flume Experiments. *Journal of*  
352 *Sedimentary Research*, 71(2), 246–254. <https://doi.org/10.1306/091400710246>
- 353 NASA. (2020). Landsat 4/5/7/8. Retrieved from <http://landsat.usgs.gov/>
- 354 Nienhuis, J. H., Ashton, A. D., Edmonds, D. A., Hoitink, A. J. F., Kettner, A. J., Rowland, J. C.,  
355 & Törnqvist, T. E. (2020). Global-scale human impact on delta morphology has led to net  
356 land area gain. *Nature*, 577(7791), 514–518. <https://doi.org/10.1038/s41586-019-1905-9>
- 357 Nittrouer, J. A., & Viparelli, E. (2014). Sand as a stable and sustainable resource for nourishing  
358 the Mississippi River delta. *Nature Geoscience*, 7(5), 350–354.  
359 <https://doi.org/10.1038/ngeo2142>
- 360 Oppenheimer, M., Glavovic, B. C., Hinkel, J., van de Wal, R. S. W., Magnan, A. ., Abd-  
361 Elgawad, A., ... Sebesvari, Z. (2019). Sea Level Rise and Implications for Low-Lying  
362 Islands, Coasts and Communities. In H. O. Portner, D. C. Roberts, V. Masson-Delmotte, P.  
363 Zhai, M. Tignor, E. Poloczanska, ... N. M. Weyer (Eds.), *IPCC Special Report on the*  
364 *Ocean and Cryosphere in a Changing Climate*. IPCC.
- 365 Paola, C., Twilley, R. R., Edmonds, D. A., Kim, W., Mohrig, D., Parker, G., ... Voller, V. R.  
366 (2011). Natural processes in delta restoration: application to the Mississippi Delta. *Annual*  
367 *Review of Marine Science*, 3(1), 67–91. [https://doi.org/10.1146/annurev-marine-120709-](https://doi.org/10.1146/annurev-marine-120709-142856)  
368 [142856](https://doi.org/10.1146/annurev-marine-120709-142856)
- 369 Pekel, J.-F., Cottam, A., Gorelick, N., & Belward, A. S. (2016). High-resolution mapping of  
370 global surface water and its long-term changes. *Nature*, 540(7633), 418–422.  
371 <https://doi.org/10.1038/nature20584>

- 372 Schuerch, M., Spencer, T., Temmerman, S., Kirwan, M. L., Wolff, C., Lincke, D., ... Brown, S.  
373 (2018). Future response of global coastal wetlands to sea-level rise. *Nature*, *561*(7722),  
374 231–234. <https://doi.org/10.1038/s41586-018-0476-5>
- 375 Shirzaei, M., Freymueller, J., Törnqvist, T. E., Galloway, D. L., Dura, T., & Minderhoud, P. S. J.  
376 (2021). Measuring, modelling and projecting coastal land subsidence. *Nature Reviews Earth*  
377 *& Environment*, *2*(1), 40–58. <https://doi.org/10.1038/s43017-020-00115-x>
- 378 Stanley, D. J., & Warne, A. G. (1994). Worldwide Initiation of Holocene Marine Deltas by  
379 Deceleration of Sea-Level Rise. *Science*, *265*(5169), 228–231.  
380 <https://doi.org/10.1126/science.265.5169.228>
- 381 Swenson, J. B. (2005). Fluviodeltaic response to sea level perturbations: Amplitude and timing  
382 of shoreline translation and coastal onlap. *Journal of Geophysical Research*, *110*(F3),  
383 F03007. <https://doi.org/10.1029/2004JF000208>
- 384 Syvitski, J. P. M., Vorosmarty, C. J., Kettner, A. J., & Green, P. (2005). Impact of Humans on  
385 the Flux of Terrestrial Sediment to the Global Coastal Ocean. *Science*, *308*(5720), 376–380.  
386 <https://doi.org/10.1126/science.1109454>
- 387 Syvitski, J. P. M., & Saito, Y. (2007). Morphodynamics of deltas under the influence of humans.  
388 *Global and Planetary Change*, *57*(3–4), 261–282.  
389 <https://doi.org/10.1016/j.gloplacha.2006.12.001>
- 390 Thieler, E. R., Pilkey, O. H., Young, R. S., Bush, D. M., & Chai, F. (2000). The use of  
391 mathematical models to predict beach behaviour for US coastal engineering: a critical  
392 review. *Journal of Coastal Research*, *16*(1), 48–70.
- 393 Vousdoukas, M. I., Ranasinghe, R., Mentaschi, L., Plomaritis, T. A., Athanasiou, P., Luijendijk,  
394 A., & Feyen, L. (2020). Sandy coastlines under threat of erosion. *Nature Climate Change*,  
395 *10*(3), 260–263. <https://doi.org/10.1038/s41558-020-0697-0>
- 396 Ward, P. J., Winsemius, H. C., Kuzma, S., Bierkens, M. F. P., Bouwman, A., Moel, H. DE, ...  
397 Luo, T. (2020). Aqueduct Floods Methodology. *World Resources Institute*, (January), 1–28.  
398 Retrieved from [www.wri.org/publication/aqueduct-floods-methodology](http://www.wri.org/publication/aqueduct-floods-methodology)

399 Wolinsky, M. A. (2009). A unifying framework for shoreline migration: 1. Multiscale shoreline  
 400 evolution on sedimentary coasts. *Journal of Geophysical Research*, 114(F1), F01008.  
 401 <https://doi.org/10.1029/2007JF000855>

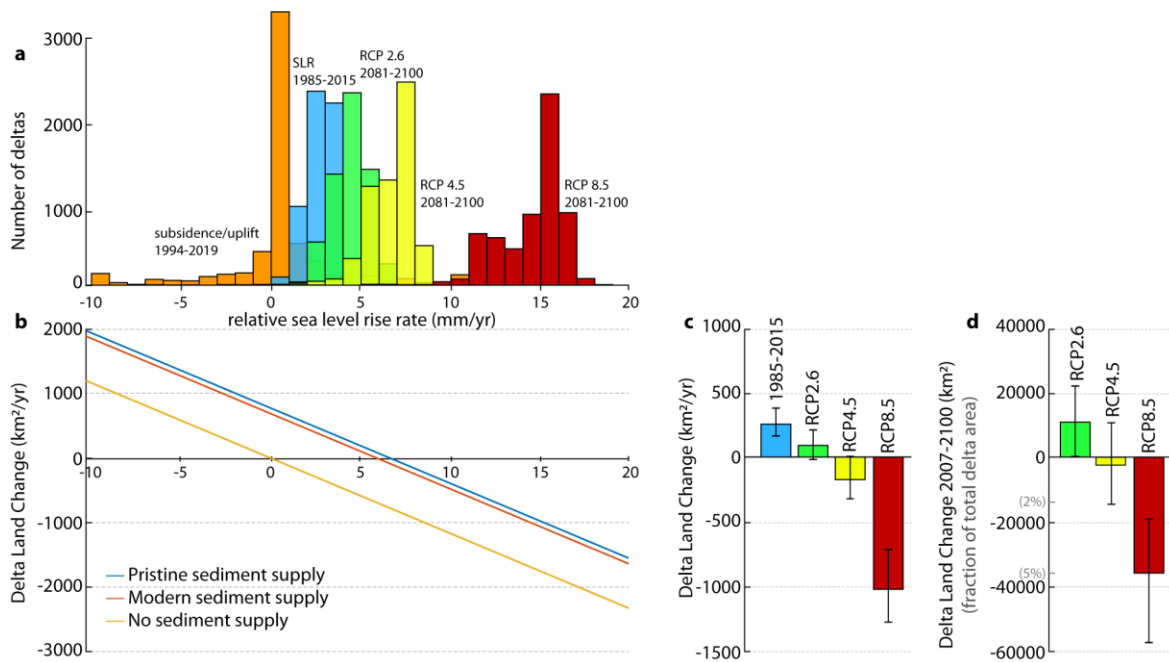


402  
 403 **Figure 1: Delta profile response to relative sea-level rise.** Model schematization for (a) delta  
 404 land gain, and (b) delta land loss, including notation used in equation (1), and (c) locations of  
 405 deltas, and (d) longitudinal profiles of 6,402 coastal deltas included in this study.



406  
 407 **Figure 2: Predicted vs. observed delta area change for individual deltas,** where the marker size  
 408 scales with the fluvial sediment flux.

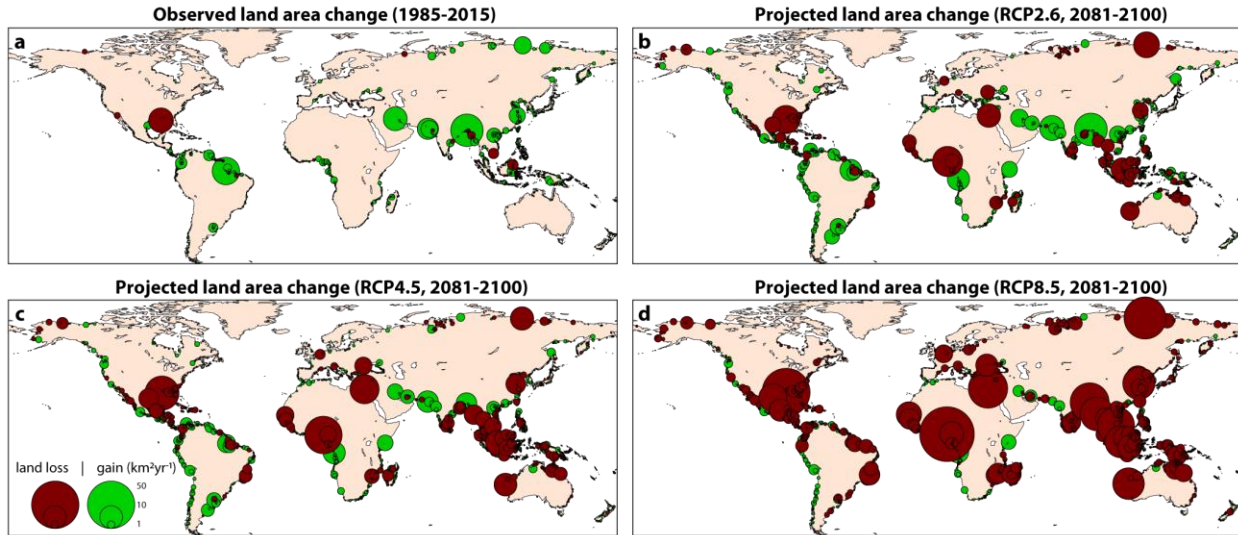
409



410

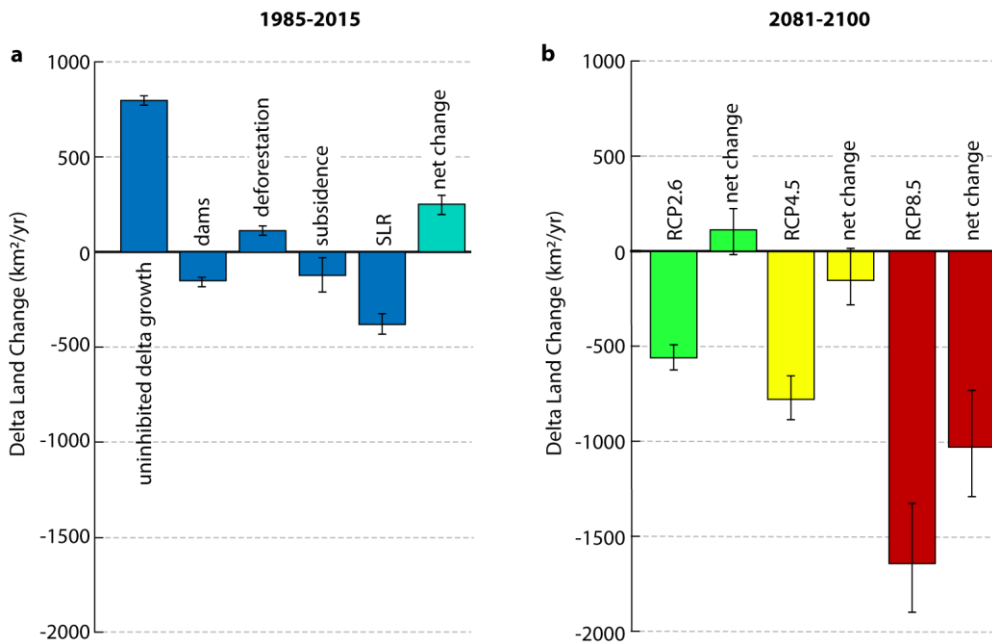
411 **Figure 3: Effect of sea-level rise on delta land change.** (a) Histogram of subsidence and sea-  
 412 level rise rates for all coastal deltas (Dangendorf et al., 2019; Oppenheimer et al., 2019; Shirzaei  
 413 et al., 2021). Note that subsidence extends beyond the axis range, in part because these data are  
 414 not available for most deltas. (b) Effect of sea-level rise rates on global delta land change for  
 415 various fluvial sediment supply scenarios. (c) and (d) Land area change of all coastal deltas for  
 416 past and projected RSLR, including subsidence for (c) 2081-2100 and (d) cumulative from 2007-  
 417 2100.

418



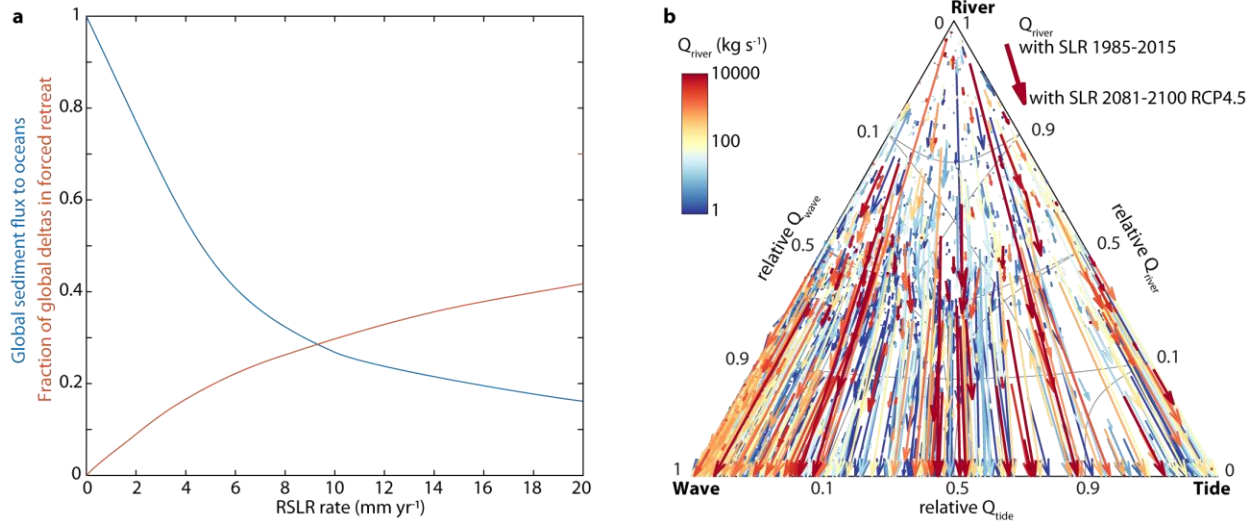
419

420 **Figure 4: Spatial variability of delta land-area change**, based on (a) observations and (b, c, d)  
 421 projections of RSLR under RCP 2.6, 4.5, and 8.5. Contribution of coastal subsidence to RSLR is  
 422 included in the land area change projections.



423

424 **Figure 5: Relative influence of human drivers on delta change.** Effect of different drivers of  
 425 sediment supply or RSLR on delta growth, resulting in (a) net observed land gain from 1985-  
 426 2015, and (b) projections of future delta change if the influence of dams, deforestation, and  
 427 subsidence remain the same.



428

429 **Figure 6: Effect of RSLR on delta morphology.** (a) Effect of RSLR on (in blue) the global  
 430 fluvial sediment flux to deltaic river mouths and (in red) the fraction of all coastal deltas (n =  
 431 6,402) where the river mouth is abandoned, and no fluvial sediment reaches the river mouth. (b)  
 432 Effect of the reduced sediment flux to the river mouth on delta morphology, comparing modern  
 433 SLR to SLR under RCP4.5 by 2100. Ternary diagram indicates relative influence of wave-, tidal-  
 434 and fluvial sediment flux on delta morphology (Nienhuis et al., 2020).